Chapter 9
Oscillating Load-Induced Acoustic Emission in Laboratory Experiment

A. Ponomarev, D. Lockner, S. Stroganova, S. Stanchits, and V. Smirnov

Abstract Spatial and temporal patterns of acoustic emission (AE) were studied. A pre-fractured cylinder of granite was loaded in a triaxial machine at 160 MPa confining pressure until stick-slip events occurred. The experiments were conducted at a constant strain rate of 10^{-7} s^{-1} that was modulated by small-amplitude sinusoidal oscillations with periods of 175 and 570 seconds. Amplitude of the oscillations was a few percent of the total load and was intended to simulate periodic loading observed in nature (e.g., earth tides or other sources). An ultrasonic acquisition system with 13 piezosensors recorded acoustic emissions that were generated during deformation of the sample. We observed a correlation between AE response and sinusoidal loading. The effect was more pronounced for higher frequency of the modulating force. A time-space spectral analysis for a "point" process was used to investigate details of the periodic AE components. The main result of the study was the correlation of oscillations of acoustic activity synchronized with the applied oscillating load. The intensity of the correlated AE activity was most pronounced in the "aftershock" sequences that followed large-amplitude AE events. We suggest that this is due to the higher strain-sensitivity of the failure area when the sample is in a transient, unstable mode. We also found that the synchronization of AE activity with the oscillating external load nearly disappeared in the period immediately after the stick-slip events and gradually recovered with further loading.

A. Ponomarev (✉) and S. Stroganova
Schmidt Institute of Physics of the Earth, Russian Academy of Sciences, Moscow, Russia
e-mail: avp@ifz.ru

D. Lockner
USGS, Menlo Park, CA, USA

S. Stanchits
GFZ, Potsdam, Germany

V. Smirnov
Schmidt Institute of Physics of the Earth, Russian Academy of Sciences, Moscow, Russia
Moscow State University, Moscow, Russia

V. de Rubeis et al. (eds.), *Synchronization and Triggering: from Fracture to Earthquake Processes*, GeoPlanet: Earth and Planetary Sciences 1,
DOI 10.1007/978-3-642-12300-9_9,

Cosmic and meteorological forces can produce periodic changes in the Earth's crust. This periodicity in terrestrial processes is observed over a wide range of time scales [Atlas. . ., 1998; 2002]. Seismicity, for example, contains periodic components as well as random activity, due to both natural and man-made sources [Gomberg et al., 1998]. Earth tides are a significant source of periodic stress and deformation of the crust and under favorable conditions can influence the occurrence of earthquakes [Cochran et al., 2004]. Sadovsky et al. [1981] have shown that micro-mechanical influence on deformed samples of different rock and artificial materials favors the transformation from brittle rupture to plastic deformation and thereby leads to release of elastic energy stored in the sample. Sobolev et al. [1996] have shown in laboratory experiments on granite blocks under biaxial loading that the addition of vibrational loads leads to a shortening of the time period between consecutive unstable motions like stick-slip. Under 50 MPa confining pressure, a strong correlation between the periodic forcing function and the occurrence of model earthquakes was found by using granite cylinders containing precut bare fault surfaces [Lockner and Beeler, 1999]. More recently, those researchers demonstrated on laboratory-scale experiments that seismicity should correlate strongly with the amplitude and frequency of small periodic stress of tidal magnitude if the period exceeds the duration of earthquake nucleation [Beeler and Lockner, 2003].

The objective of the current study was to analyze acoustic emission time series (considered an analogue of natural seismicity) generated in laboratory-scale experiments to reveal variations in the sensitivity between periodic loading and induced AE response. Unlike the preceding experiments, we used a pre-fractured Westerly granite core of 76.2 mm diameter and 190 mm height under confining pressure of 160 MPa (Fig. 9.1). The sample was loaded axially until stick-slip events occurred. The experiments were carried out under constant strain rate of 10^{-7} s^{-1}. The steady axial loading was modulated by sinusoidal oscillations of 175 and 570 second periods and with peak-to-peak amplitudes that were a few percent of the applied load. This loading pattern was intended to simulate periodic loading observed in nature (e.g., earth tides or other sources), although the stress variations are more than 3 orders of magnitude larger than tidal stress oscillations. As discussed in Lockner and Beeler [1999], correlations between tidal stresses and natural seismicity are expected to be much smaller than the correlations observed in this experiment. An ultrasonic acquisition system described in Lockner et al. [1991], included 13 piezosensors and recorded arrival time and amplitude information from induced AE events to provide a database for further analysis.

Loading history and variation of AE activity are shown in Fig. 9.2. The initial stage of the experiment (before 310,000 s) was loaded at constant strain rate without the addition of periodic forcing. In the range of 310,000-360,000 s, the constant loading rate was modulated by the addition of a small-amplitude sine-wave with a period of 175 s. In the range of 375,000 to 445,000s, the period of the modulating signal was 570 seconds. The amplitude of the periodic loading was approximately 20 MPa in both cases.

Artificial fault surfaces used in laboratory studies are typically formed by making an inclined saw cut that is surface ground to produce planar, well-mated

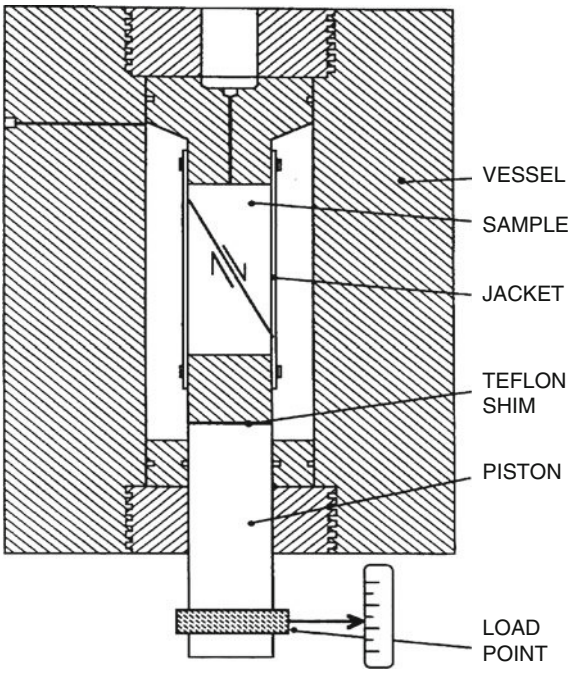

Fig. 9.1 Schematic diagram of the loading system (after Lockner and Beeler, 1999)

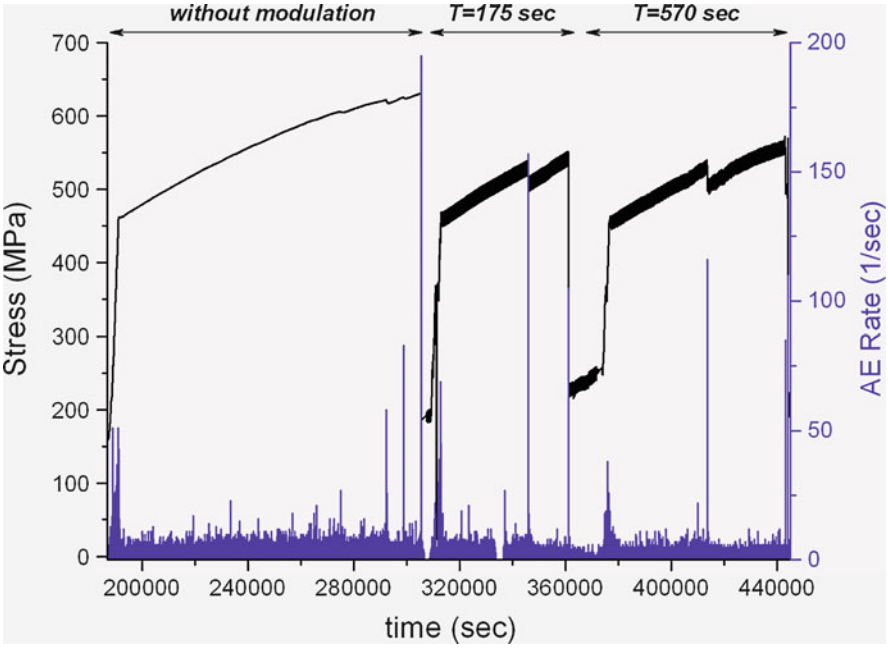

Fig. 9.2 Axial load and recorded AE rate are plotted as a function of time. Broad bands in axial stress between 500 and 600 MPa indicate amplitude of imposed sinusoidal stress oscillations

surfaces. A different technique was employed here to produce a more 'natural' fault surface. In a separate procedure, before the experiment, a fracture was propagated quasi-statically in an initially intact granite cylinder. An "AE feedback control" technique was used in which the load was adjusted to maintain constant acoustic activity [Lockner et al., 1991]. This loading style results in a narrow rupture zone with complex surface roughness and abundant gouge that is more like a natural fault than an artificial saw-cut surface. Locations of AE sources generated from initial loading to 200,000 s are plotted in Fig. 9.3. These events, that have location accuracy of approximately ±3mm, are the result of re-activation of the existing fault surface and provide an image of its shape. While AE activity is greater in the central portion of the fault, there is activity over the entire fault surface. This distributed activity indicates that during reloading of this pre-fractured sample, the entire fault surface is reactivated and although the two fault blocks are locked together by the applied normal stress (up to 260 MPa) a small amount of inelastic strain is continuously occurring. The AE activity plotted in Fig. 9.3a indicates that the lower portion of the fault has slight curvature and that the damage zone associated with the fault is more than 1 cm in width.

Dynamic stick-slip events involve rapid motion on the entire fault surface accompanied by a measurable stress drop and audible sound. Only a few such stick-slip events occurred during this experiment and all were followed by periods of increased AE activity. Variation in the relevant acoustic activity is shown in Fig. 9.4 for two stick-slip events with differential stress drops of approximately

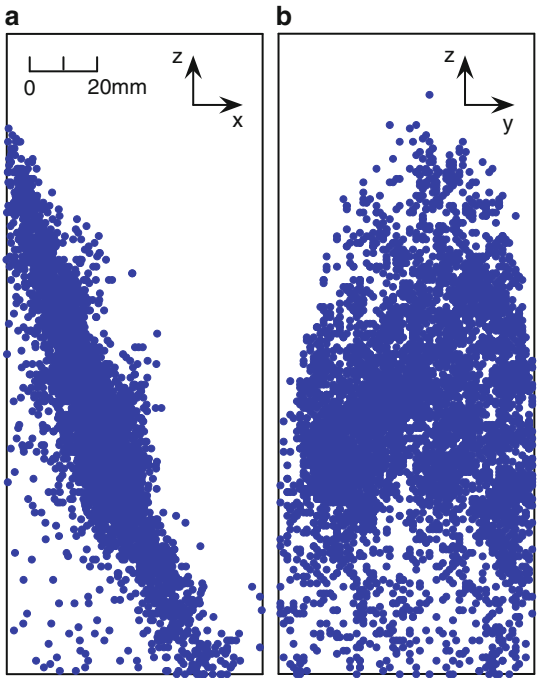

Fig. 9.3 Locations of AE events during initial loading (before running time of 200,000 s) of sample. **(a)** Sample viewed along strike of the pre-existing fault. **(b)** Sample view rotated 90° to fault strike. Lower portion of the fault has slight curvature. Width of the damage zone, as indicated by AE activity, is more than 1 cm. The broadly distributed AE activity indicates that the entire fault is undergoing inelastic strain as it is loaded

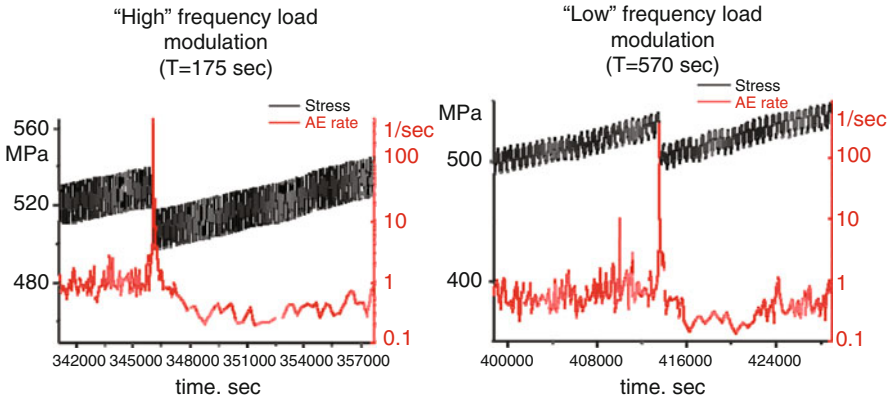

Fig. 9.4 Acoustic activity associated with stick-slip events. Steady loading rate results in an average AE rate of about 10 events per second. Rapid fluctuations in the AE rate prior to stick-slip events indicates the response to applied stress oscillations. Each stick-slip event produces a sudden increase in AE rate followed by a 1/time 'aftershock' decay and a 'stress shadow' where AE rate drops to about 30% of the previous rate. During the aftershock decay, the correlation between AE rate and stress oscillations is lost

20 MPa. In both examples shown in Fig. 9.4, AE activity preceding stick-slip was strongly correlated with the imposed stress oscillations. However, synchronization of acoustic emission nearly disappears following the stick-slip events and the associated stress drops. Then, after about 10,000 seconds, as the load rises, the correlation between AE rate and periodic loading rate is gradually re-established. Stress drops for the different stick-slip events were variable. The two events shown in Fig. 9.4 had stress drops of approximately 20 MPa or only about 4 percent of the applied differential stress. These stress drops were of the same magnitude as the applied stress modulations. Notice in Fig. 9.4 that the decrease in ambient stress level due to the stick-slip events resulted in an overall ½ decade decrease in AE rate during the aftershock sequence that reached a minimum after about 5000 s. This inverse-time transient decay in AE rate is the laboratory equivalent of an Omori aftershock decay sequence and represents the time period in which AE rate is insensitive to the imposed stress oscillations. Once the sample emerges from this region of lowered stress, the AE rate again begins to correlate with the imposed stress oscillations. This memory of past stress history is similar to the Kaiser effect discussed, for example, in Lockner (1993) in which the induced AE rate remains low until the previous maximum stress level is exceeded.

The change in correlation between stress oscillations and AE rate is shown more clearly in Fig. 9.5. In these plots, AE activity occurring within an extended time interval is binned according to time of occurrence relative to the peak in the stressing cycle. Fig. 9.5a shows that in a 10,000 s interval prior to the stick-slip event in Fig. 9.4a, AE activity has a strong correlation with and is in phase with the stress oscillations. The number of AE events associated with peak stress is nearly 3 times more than the number of events occurring near the stress minimum. Plotted

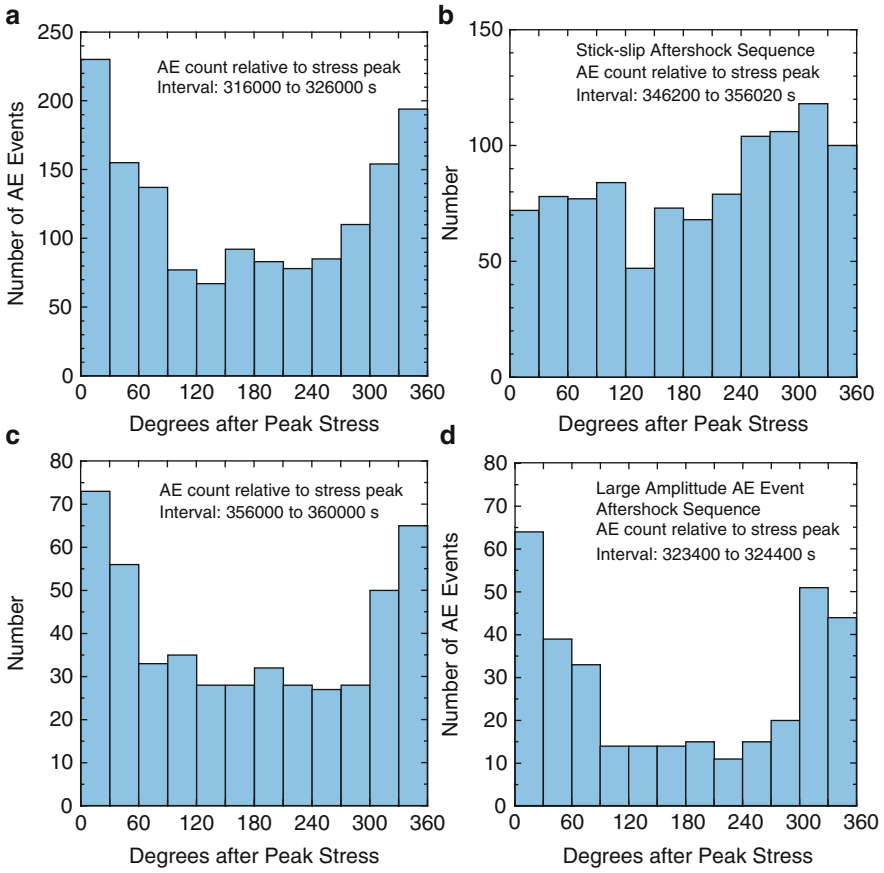

Fig. 9.5 AE activity plotted relative to the peak in each stressing cycle (T = 175 sec). Events for each sampling interval are grouped in 30° bins. **(a)** AE activity for 10,000 sec time interval before stick-slip event shown in Fig. 9.4a. Activity at peak stress is nearly 3 times as large as activity near stress minimum. **(b)** AE activity during 10,000 sec following stick-slip event showing a loss of correlation with stress cycling. **(c)** Activity during 4000 sec time interval following aftershock sequence of stick-slip event. In this interval, the correlation between stress and AE rate is re-established. **(d)** AE activity for 1000 sec aftershock sequence of a large amplitude AE event (see text). In this case, correlation of AE activity with stress oscillations is greater than for the background activity shown in Fig. 9.5a

in this way, Fig. 9.5a approximates the probability density function for AE events in this time interval. In contrast, Fig. 9.5b plots the AE activity during the 10,000 s following the stick-slip event. The correlation between stress and AE rate is essentially lost. However, in the next 4,000 s (Fig. 9.5c) the correlation between peak stress and peak AE rate is re-established.

Another interesting feature of induced acoustic emission is that AE synchronization with external loading becomes apparent following large amplitude AE events (events that are large enough to have their own aftershock sequences).

This is illustrated in Fig. 9.6. Similar to the aftershock sequence for stick-slip events, these large AE event aftershocks diminish with an inverse-time rate dependence. Unlike stick-slip aftershocks, however, aftershocks of large AE events show strong correlation with stressing cycles. This characteristic is further illustrated in Fig. 9.5d where the peak activity is more than 4 times the activity associated with the stress minimum.

We suggest that the appearance of strong synchronization between imposed stress oscillations and acoustic emission variations during laboratory-scale modeling is the result of increased strain-sensitivity of the fault and indicates that the fault has been driven into an unstable state. In Fig. 9.4, the stick-slip events involved slip of the entire fault surface and resulted in an overall reduced stress state as measured by

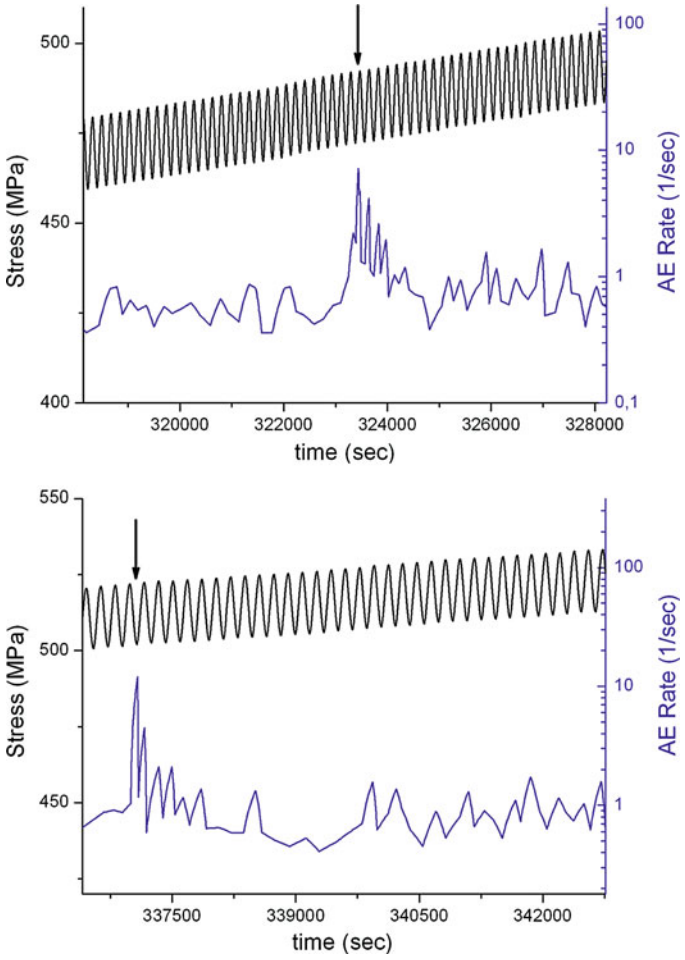

Fig. 9.6 Acoustic activity synchronizes with applied stress oscillations after large amplitude acoustic events that occur at times indicated by arrows. Interval of enhanced correlation is approximately 1000 sec

the applied axial load. This reduced stress state was characterized by a loss of correlation between AE rate and imposed stress oscillations. In contrast, in Fig. 9.6, while the AE events were large enough to produce their own aftershock sequences, they did not reduce the overall stress on the fault as measured by the total applied axial load. Instead, the drop in stress in the source region of the large AE events simply transferred stress to the remainder of the fault surface resulting in a transient increase in overall AE rate.

More than 65,000 AE events were recorded and located during this experiment. AE activity associated with the stick-slip event at 346,023 sec is plotted in Fig. 9.7. A very large amplitude AE event was recorded at the beginning of the aftershock sequence (plotted as the star in circle) and may indicate the nucleation site of the stick-slip event [Thompson et al., 2005]. Differences between locations of pre-stick-slip AE and aftershocks are small. Activity in regions 'A' and 'B' decreased while activity in 'C' increased. These changes may indicate evolution of highly stressed zones or asperities due to fault slip. Otherwise, the broad distribution of AE both before and after the stick-slip event indicates that the entire fault is stressed and undergoing inelastic deformation. Figure 9.8 shows locations of AE events before and after the large amplitude AE event described in Fig. 9.6a. The large event, indicated by the star, occurred near the center of the sample. Once again, there is little difference in location of preceding and immediately following the large amplitude AE event. Apparently, the occurrence of the large event resulted in a sudden increase in AE activity but not in a change in the spatial distribution of activity, implying a relatively uniform increase in stress over the entire fault surface.

$$\lambda(t) = \mu \cdot (1 + a \cdot \cos(\omega t + \varphi))$$

We employ a method described by Lyubushin et al. [1998] to extract the periodic component from the AE time series that represents a 'point' process. The model of acoustic intensity includes a Poisson process with a uniform purely random part with intensity μ (μ>0) and a periodic component (frequency ω, amplitude a ($0 \leq a \leq 1$) and phase φ). Thus the Poisson part of the intensity is modulated by a harmonic oscillation.

The log-likelihood function for the set of observations is defined as

$$\ln L(\mu, a, \varphi|\omega) = \sum_{t_i} \ln(\lambda(t_i)) - \int_0^T \lambda(s)ds$$

and the increment of the log-likelihood function becomes

$$\ln L(\mu_i, a, \varphi|\omega) = \sum_{t_i} \ln(1 + a\cos(\omega t_i + \varphi)) + N \cdot \ln(\mu_i, a, \varphi|\omega)) - N$$

$$\Delta \ln L(a, \varphi|\omega) = \sum_{t_i} \ln(1 + a\cos(\omega t_i + \varphi)) + N \cdot \ln(\mu_i, a, \varphi|\omega))$$

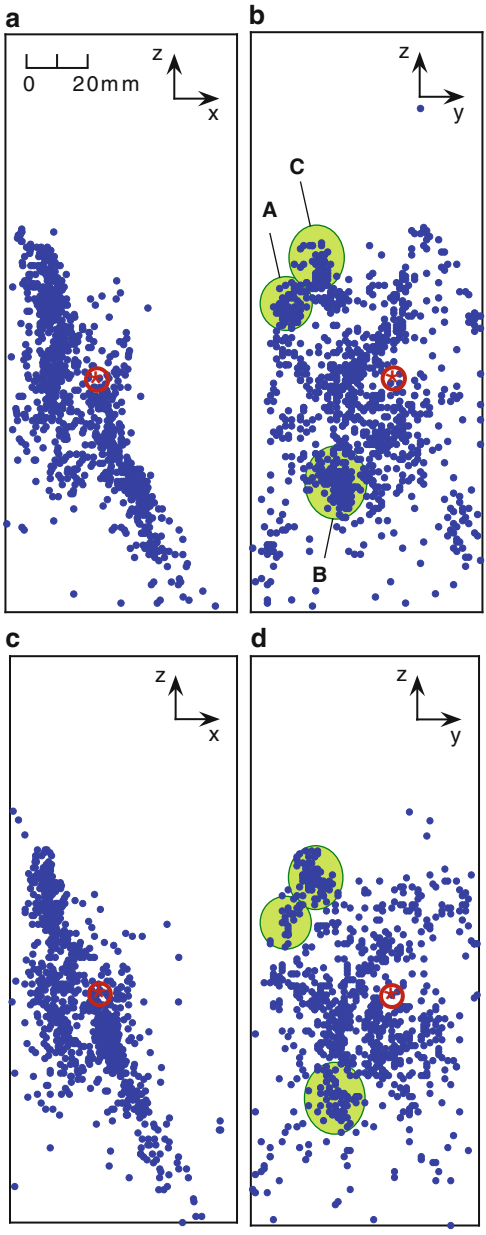

Fig. 9.7 Plots of AE activity associated with stick-slip event at 346,023 s running time. **(a)** and **(b)** show locations of events in 10,000 s interval before the stick-slip. **(c)** and **(d)** show aftershocks occurring for 10,000 s following the stick-slip. Star in circle indicates location of an off-scale amplitude AE event that coincides with the time of the stick-slip and may represent its nucleation site. Groups of events 'A', 'B', and 'C' show a change in relative activity from before to after the stick-slip and may reflect evolution of the fault surface due to co-seismic slip

The maximum of this function indicates which frequencies provide the greatest increase in the log-likelihood function when compared to a purely random model. Parameters a and ω can be estimated.

A time-frequency diagram of the AE response (log-likelihood increments) for the entire experiment is shown in Fig. 9.9. Horizontal red lines identify the portions

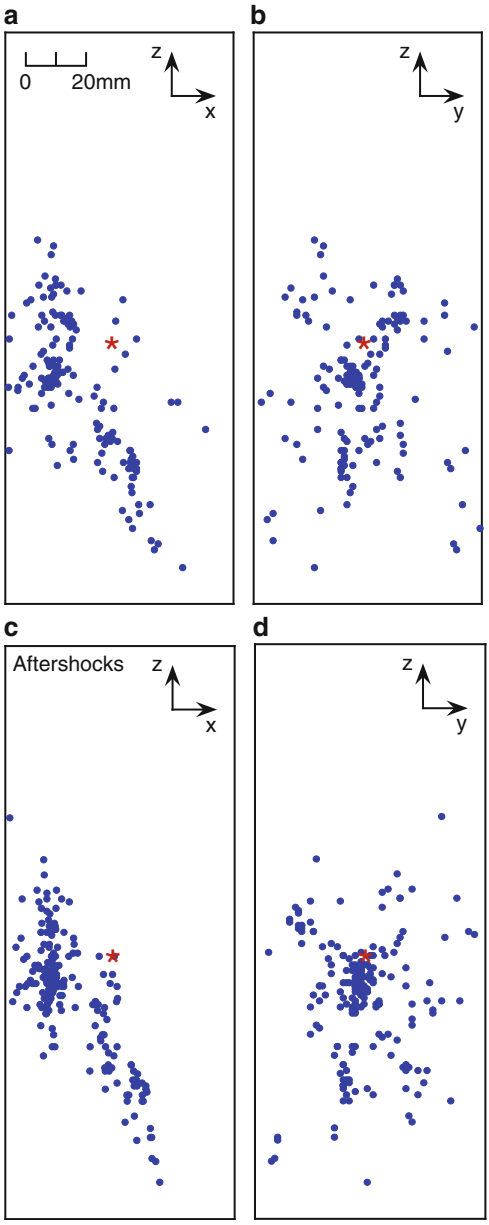

Fig. 9.8 Plots of AE activity associated with the large amplitude AE event described in Fig.6a at 323,377 sec running time. Location of this event is indicated by star. **(a)** and **(b)** Location of events occurring 2000 sec before the large AE. **(c)** and **(d)** Location of aftershock events occurring for 1000 sec following the large AE. Spatial distribution of AE events does not appear to be affected by the occurrence of the large event. Only the AE rate increased, suggesting that the large event redistributed stress relatively uniformly over the entire fault surface

of the experiment in which the AE response had periodicity of 175 s (logT = 2.24) and 570 s (logT = 2.75).

There is no periodic acoustic response during the initial stage of the experiment because no sinusoidal load is added to the constant loading rate. In general, a correlation between the sinusoidal loading and the AE response is observed over

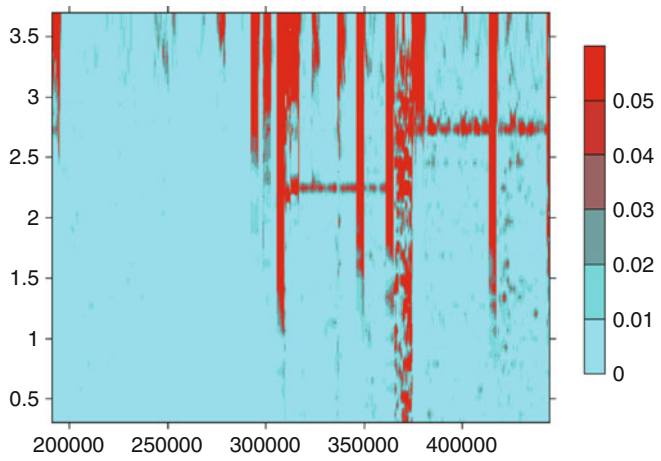

Fig. 9.9 Plot of the log-likelihood function for the entire experiment. Light-grey background indicates essentially random occurrence of AE activity. Dark regions indicate high values of log-likelihood function. Horizontal red bands during second half of the experiment indicate periods where AE activity correlates with the periodic stressing function. Vertical streaks are typically the result of rapid stress changes, including stick-slip events

the next part of the experiment. However, the magnitude of the response is not stable – sometimes it becomes very small and almost disappears. This effect is seen by a detailed examination of spectral-temporal diagrams (Fig. 9.10). Wide vertical stripes of the high values of the log-likelihood function are the result of an abrupt increase or decrease of acoustic activity due to rapid unloading of the sample, including stick-slip events.

From this preliminary analysis we can draw the following conclusions.

1) Prior to stick-slip events that represent dynamic failure of the entire fault surface, the AE rate correlates with the applied stress oscillations (periods of 175 s and 570 s). Omori-type aftershock sequences of these events lasted for a few thousand seconds. During these time intervals, AE activity did not correlate with the imposed stress oscillations. As AE activity increased due to reloading of the sample following the co-seismic stress drop and aftershock decay, AE rate again correlated with the imposed stress oscillations.
2) 'Significant' large-amplitude AE events were identified that produced Omori-type aftershock AE activity but did not involve slip of the entire fault surface or a drop in average stress. In this case, the aftershock activity showed an increased correlation with imposed oscillating stress.
3) These observations are consistent with a model in which AE activity becomes increasingly sensitive to stress perturbations as the stress level in the sample is raised and the fault is driven close to failure. If this is a general property of natural fault systems, it may be possible to identify instability and impending failure by the response of the fault to periodic stressing. It would seem reasonable to search for these effects during real aftershock series.

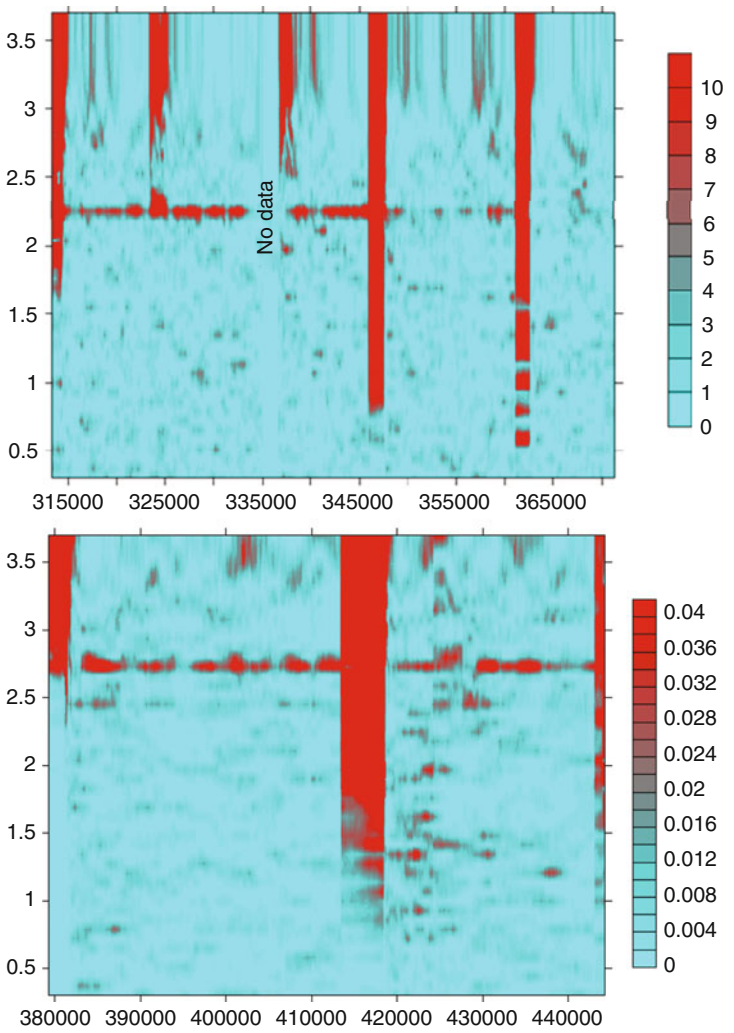

Fig. 9.10 Log-likelihood plots showing detailed segments of the experiment. Stick-slip events shown in Fig. 9.4 occur at 346,027 and 413,528 s running time and are followed by aftershock sequences with no distinct correlation to stress oscillations

References

Atlas of temporal variations of natural, antropogenic and social processes. V.2. M., Scientific World. 432 p., 1988 (in Russian).

Atlas of temporal variations in natural, antropogenic and social processes. V.3. M., Janus-K, 676 p., 2002 (in Russian).

Beeler, N. M., and D. A. Lockner. Why earthquakes correlate weakly with the solid Earth tides: Effects of periodic stress on the rate and probability of earthquake occurrence, J. Geophys. Res., 108(B8), 2391, doi:10.1029/2001JB001518, 2003.

Cochran, E. S, J. E. Vidale and S. Tanaka. Earth tides can trigger shallow thrust fault earthquakes, Science, 306, 1164–1166, 2004.

Gomberg, J., N. M. Beeler, M. L. Blanpied, and P. Bodin. Earthquake triggering by transient and static deformations, J. Geophys. Res., 103, 24411 –24426, 1998.

Lockner, D. A., and N. M. Beeler. Premonitory slip and tidal triggering of earthquakes, J. Geophys. Res., 104, 20133–20151, 1999.

Lockner, D. A.. The role of acoustic emission in the study of rock fracture, Int. J. Rock Mech. Min. Sci. Geomech. Abstr., 30, 883–899, 1993.

Lockner, D. A., J. D. Byerlee, V. Kuksenko, A. Ponomarev, and A. Sidorin. Quasi-static fault growth and shear fracture, Nature, 350, 39–42, 1991.

Lyubushin A.A., V.F.Pisarenko, V.V.Ruzich and V.Yu.Buddo. A New method for identifying seismicity periodicities – Volcanology and Seismology, vol.20, 1998, pp. 73–89.

Sadovsky M.A., Mirzoev K.N, Negmatullaev S.Kh., Salomov N.G. Influence of mechanical microoscillations on the feature of material plastic strain. Solid Earth, N 6, 1981, 32–42, 1981 (in Russian).

Sobolev G.A., Ponomarev A.V., Koltzov A.V. and Smirnov V.B. Simulation of triggering earthquakes in the laboratory. PAGEOPH, v.147, N 2, 1996, p.345–355.

Thompson, B. D., R. P. Young and D. A. Lockner, Observations of premonitory acoustic emission and slip nucleation during a stick slip experiment in smooth faulted Westerly granite, Geophys. Res. Lett., 32, doi:10.1029/2005GL022750, 2005.